JAIST Repository
https://dspace.jaist.ac.jp/

Title	Nanostructured assembly of porphyrin clusters for light energy conversion
Author(s)	Hasobe, Taku; Imahori, Hiroshi; Fukuzumi, Shunichi; Kamat, Prashant V.
Citation	Journal of Materials Chemistry, 13(10): 2515-2520
Issue Date	2003
Type	Journal Article
Text version	author
URL	http://hdl.handle.net/10119/7906
Rights	Copyright (C) 2003 Royal Society of Chemistry. Taku Hasobe, Hiroshi Imahori, Shunichi Fukuzumi and Prashant V. Kamat, Journal of Materials Chemistry, 13(10), 2003, 2515-2520. http://dx.doi.org/10.1039/b306871d - Reproduced by permission of The Royal Society of Chemistry
Description	

JAIST
JAPAN
ADVANCED INSTITUTE OF
SCIENCE AND TECHNOLOGY

Japan Advanced Institute of Science and Technology

Nanostructured assembly of porphyrin clusters for light energy conversion

Taku Hasobe,[a,b] Hiroshi Imahori,[c,*] Shunichi Fukuzumi,[b,*]

and Prashant V. Kamat[a,*]

Notre Dame Radiation Laboratory, University of Notre Dame,

Notre Dame, IN 46556-0579

And

Department of Material and Life Science, Graduate School of Engineering,

Osaka University, CREST, Japan Science and Technology Corporation (JST),

Suita, Osaka 565-0871, Japan

And

Department of Molecular Engineering, Graduate School of Engineering,

Kyoto University, PRESTO, JAPAN Science and Technology Corporation (JST), Katsura, Nishikyo-ku, Kyoto 615-8510, Japan and Fukui Institute for Fundamental Chemistry, Kyoto University, 34-4, Takano-Nishihiraki-cho, Sakyo-ku, Kyoto 606-8103, Japan

[a]University of Notre Dame, [b] Osaka University, [c]Kyoto University

Abstract

Free base porphyrin molecules form well-defined and ordered nanoclusters in mixed solvents with absorption characteristics that significantly differ from those of the monomer form. These self-assembled crystallites in acetonitrile/toluene (9:1, v/v) can be deposited as thin films on nanostructured TiO_2 electrode using an electrophoretic technique. These porphyrin cluster assembly is highly photoactive and capable of undergoing charge separation under visible light excitation. Photoexcitation of the porphyrin film electrode assembly in a photoelectrochemical cell with visible light produces relatively high photocurrent generation. A maximum photocurrent of 0.15 mA cm^{-2} and a photovoltage of 250 mV were attained using I_3^-/I^- redox couple. The electron flow to TiO_2 electrode can be facilitated by application of a positive potential. An incident photon-to-photocurrent generation efficiency (IPCE) of 2.0 % has been achieved at an applied bias potential of 0.2 V *vs.* SCE. The broad photoresponse of these crystallites throughout the visible range as well as the ease of assembling them on the electrode surface opens up new avenues for harvesting a wide wavelength range of solar light.

Introduction

Self association or aggregation as a method of organizing molecules as clusters of controlled size and shape is a simple and convenient method to design organized assemblies.[1,2] Of particular interest is the ability of such aggregates to mimic the energy and electron transfer processes of the photosynthetic reaction center, providing better understanding of the photosynthesis.[3] Furhop et al.[4] have demonstrated that amphiphillic porphyrin aggregates in an aqueous solution in the form of fibers, ribbons and tubules. Hydrogen bonding, van der Waals interaction, and hydrophobic effects are the major driving force to achieve such ordered assembly of these molecules.[4,5]

The role of molecular aggregates as photosensitizers in color photography has been well recognized.[6] Both J- and H-type aggregates of organic dyes have been demonstrated in sensitizing TiO_2 and SnO_2 films.[7-9] We have previously highlighted the role of dye aggregates as light harvesting assemblies to gather and transfer energy to monomer dye molecules.[10-12] Larger crystallites of organic semiconductors can also undergo photoinduced charge separation and can participate in the photocurrent generation.[10-12]

As the special pair in the light-harvesting bacterial complex LH2 has the characteristic arrays of the bacteriochlorophyll,[13] efficient molecular aggregation or assembly has attracted special attention in the field of photoelectrochemistry of organic dyes.[14,15] It is well-known that porphyrin arrays linked with covalent or non-covalent bond, which have strong interactions between porphyrin chromophores, have broad absorption in all the visible light region.[16-19] Thus, porphyrin

chromophores in the form of aggregated clusters provide a convenient way to increase light absorption throughout the visible region. In this context, we developed an electrophoretic deposition technique to deposit fullerene clusters in the form of nanostructured thin film.[20]

We report herein the preparation of porphyrin clusters in mixed solvents and their assembly as nanostructured films under application of a dc electric field. The porphyrin cluster film deposited on nanostructured TiO_2 electrode shows improved light harvesting efficiency as visualized from the enhanced photocurrent generation in a photoelectrochemical cell.

Experimental Section

Electrophoretic Deposition of Porphyrin Clusters

Preparation of 5,15-bis(3,5-di-*tert*-butylphenyl)porphyrin) (H_2P) has been described elsewhere.[21] Nanostructured TiO_2 films were cast on an optically transparent electrode (OTE) by applying a colloidal solution prepared from the hydrolysis of titanium isopropxide.[22] The air dried films were annealed at 673 K. The TiO_2 film electrode (OTE/TiO_2) and an OTE plate were introduced in a 1 cm path length cuvette and they were connected to positive and negative terminals of the power supply, respectively. A known amount (~2 mL) of H_2P cluster solution in acetonitrile/toluene (9/1, v/v) was transferred to a cuvette in which the two electrodes (viz., OTE/TiO_2 and OTE) were kept at a distance of ~6 mm using a Teflon spacer. A dc voltage (500V) was applied between these two electrodes using a Fluke 415 power supply. The deposition of the film can be visibly seen as the solution becomes

colorless with simultaneous brown coloration of the TiO_2/OTE electrode (H_2P cluster coated electrode will be referred to OTE/TiO_2/$(H_2P)_n$).

The UV-visible spectra were recorded on a Shimadzu 3101 or a Cary 50 spectrophotometer. Transmission electron micrographs (TEM) of H_2P clusters were recorded by applying a drop of the sample to carbon-coated copper grid. Images were recorded using a Hitachi H600 transmission electron microscope. AFM measurements were carried out using a Digital Nanoscope III in the tapping mode.

Photoelectrochemical Measurements

Photoelectrochemical measurements were performed using a standard three-compartment cell consisting of a working electrode and Pt wire gauze counter electrode and saturated calomel reference electrode (SCE). All photoelectrochemical measurements were carried out in acetonitrile containing 0.5 mol dm^{-3} NaI and 0.01 mol dm^{-3} I_2 with a Keithley model 617 programmable electrometer. A collimated light beam from a 150 W Xenon lamp with a 370 nm cut-off filter was used for excitation of the H_2P cluster films cast on TiO_2 electrodes. A Bausch and Lomb high intensity grating monochromator was introduced into the path of the excitation beam for the selecting wavelength. A Princeton Applied Research (PAR) model 173 potentiostat and Model 175 universal programmer were used for recording I–V characteristics.

Results and discussion

Self assembly of free base porphyrin in mixed solvents

H_2P is soluble in nonpolar solvents such as toluene, but less so in polar solvents such as acetonitrile. By controlling the proper choice of polar to nonpolar solvent we can achieve a controlled aggregation in the form of nanoclusters. The ratio of polar-nonpolar mixed solvent as well as the mode of mixing is an important factor in achieving desired size and shape of H_2P clusters. In our study we employed a fast-injection method in which a concentrated solution of H_2P in toluene is syringed into a pool of acetonitrile. Such a procedure produced transparent suspension of H_2P clusters. Unless otherwise mentioned we maintained a final solvent ratio of 9:1 (v/v) acetonitrile : toluene to prepare porphyrin nanoclusters.

The absorption spectra of H_2P in neat toluene and in acetonitrole/toluene (9:1, v/v) are compared in Fig. 1.

Fig. 1

While the structure of the Q-band of H_2P clusters is maintained in the cluster form, the Soret band becomes broader compared to its monomer form. Furthermore, the relative absorbance of the Q-band compared to that of the Soret band is increased in H_2P clusters. These spectral differences indicate that the intermolecular interactions in H_2P clusters influence the electronic transitions in the Soret and Q-bands in a different way. Similar spectral differences were also highlighted for functionalized porphyrin clusters prepared in mixed solvents. [8,9]

Despite the broadening of the spectrum, little change could be seen in the λ_{max} values of the Soret and Q-bands. The blue-shift observed in these bands is less than 5

nm. In molecular assemblies of J- and H- aggregate types, a significant change in the λ_{max} value of the absorption spectrum has been observed.[8,9] Furhop et al. have also shown that the spectral shifts are sensitive to the type ordered aggregation.[4a] The anionic porphyrin, meso-tetrakis-(4-sulfonatophenyl) porphyrin dianion forms highly organized J- and H- aggregates in mixed solvents or in polymer solutions.[23]

Fig. 2 shows TEM image of H_2P cluster suspension dried on a carbon grid. As the solvent evaporates these nanoclusters form a well-defined crystallites of μm size domain. The particle size and shape is also largely dependent on the ratio of the mixed solvents. The randomness in the shape is seen for the crystallites formed from the solvent ratio of 3:1 (v/v) acetonitrile:toluene (Fig. 2a). The electron micrograph shows a sample of spherical and cylindrical shapes of crystallites. On the other hand the clusters from the solvent mixture of 9:1 (v/v) acetonitrile:toluene solution produce fairly uniform size crystallites (Fig. 2b). Upon closer examination one can reveal that these crystallites are flat with a hexagonal symmetry. The hydrophobic moiety of the porphyrin moiety facilitates π-stacking, thus enabling a two dimensional growth during crystallization.

Fig. 2

It should be noted that the H_2P clusters prepared in mixed solvents are smaller in dimension, and they form larger crystallites upon drying on a copper grid. As solvent evaporates on the grid, the secondary aggregation occurs in an orderly fashion to form large crystallites. These images demonstrate that porphyrin molecules form aggregated

clusters,[24-28] which have strong intermolecular interactions in the mixed solvent. These optically transparent clusters are stable at room temperature and they can be transformed back to the monomeric form by diluting them with toluene.

Electrophoretic deposition of porphyrin aggregates

Unlike the slow evaporation of the cluster suspension on a copper grid (as described in the previous section) electrophoresis provides a quick assembly of clusters with no significant cluster growth. We demonstrated this principle earlier while depositing fullerene clusters on an electrode surface under the application of a dc field.[20] We adopted similar procedure to assemble H_2P clusters on a conducting glass electrode or OTE/TiO_2 electrode using an electrodeposition method. Under application of a dc electric field (500 V), H_2P clusters in acetonitrile/toluene (9:1, v/v) become negatively charged as they are driven towards the positively charged electrode surface. At a lower dc voltage (< 450 V), the deposition hardly occurred. With increasing time of deposition, the electrode turns brown in color exhibiting a visual demonstration of deposition process. We can also follow the growth of deposition by recording the absorption spectrum of the transparent electrode at different times of dc field application (Fig. 3). The absorbance of H_2P clusters deposited in the form of film increases with increasing the deposition time while maintaining the overall spectral shape of the Soret and Q-bands. This further ascertains the fact that the H_2P clusters are assembled on the electrode surface in an orderly fashion with no further changes in the aggregation. The inset shows the growth process as monitored from the absorption at 410 nm. It is evident from this growth trace that the deposition process can be completed in less than 10 minutes.

Fig. 3

The spectrum in the Q band region exhibits a very broad absorption band due to the intermolecular interactions in closely packed clusters of H_2P film on OTE/TiO_2.[7-9] During the deposition of H_2P clusters we also observe a small red-shift in the absorption spectrum. The λ_{max} value of OTE/TiO_2/$(H_2P)_n$ obtained at the electronic deposition time of 10 min is slightly red-shifted by 3 nm compared to the absorption spectrum recorded after 0.5 min deposition time. Such a red-shift may be due to the aggregation of H_2P on OTE/TiO_2, which enables to harvest visible light more widely across the visible light region.

The AFM image of electrophoretically deposited H_2P film (OTE/TiO_2/$(H_2P)_n$) is shown in Fig. 4a. A closely packed assembly of H_2P clusters shows the usefulness of electrophoretic deposition in providing nanoporous morphology to the film. Such a nanoporous morphology also yields a high surface area to the (OTE/TiO_2/$(H_2P)_n$) film.

Fig. 4

These films are quite robust and can be washed with polar organic solvents. A 3-D AFM image in Fig. 4b further ascertains the nanostructured morphology of the OTE/TiO_2/$(H_2P)_n$ has an uniform thin film. A close packing of these clusters on TiO_2 film is important for obtaining an efficient light harvesting photoelectrode.

From the AFM image in Fig. 4a and b it is evident that the H_2P film consists of fairly uniform size clusters with 50-100 nm diameter size. This size domain is also consistent with the particle size obtained from light scattering analysis of porphyrin cluster suspensions. This clearly shows that during the electrophoretic deposition we are able to deposit the clusters without significant growth in particle size. On the other hand the electron micrographs shown in Fig. 2 indicates formation of well-defined microcrystallites. These results demonstrate that the mode of deposition of H_2P is an important player in obtaining the desired morphology of the nanostructured film. If one desires to have a large surface area composed of small size clusters, as in the case of a photosensitive electrode, it is desirable to quickly freeze these clusters in the form of film (e.g., by employing electrophoretic deposition technique). In contrast to this quick deposition technique under the influence of a dc electric field, slow evaporation of the solvent results in yielding ordered larger size crystallites. Hence it is important to pay attention to the deposition technique as they control the overall morphology of the H_2P cluster film on electrode surfaces.

Photocurrent generation

In order to evaluate the light energy harvesting aspects of H_2P cluster films, we assembled a photoelectrochemical cell with OTE/TiO_2/$(H_2P)_n$ as the photoanode. Photocurrent measurements were carried out in acetonitrile containing I_3^-/I^- redox couple (0.5 mol dm^{-3} NaI and 0.01 mol dm^{-3} I_2) using visible light excitation ($\lambda >$ 370 nm). Fig 5a shows the reproducible photocurrent response to the ON/OFF cycles of illumination.

Fig. 5

In the presence of I_3^-/I^- redox couple, a fairly good stability in the photocurrent was achieved. The short circuit photocurrent density is 0.15 mA/cm^2, and open circuit voltage is 250 mV under visible light irradiation (110 mW/cm^2). Blank experiments conducted with OTE/TiO_2 did not produce any detectable photocurrents under similar illumination conditions.

Fig. 5b shows the I-V characteristics of OTE/TiO_2/$(H_2P)_n$ electrodes under the visible light illumination. A stable anodic photocurrent generation is seen at applied potentials greater than -0.5 V *vs.* SCE. With increasing positive bias the photocurrent increases. The application of positive bias makes the charge separation and charge transport in the OTE/TiO_2/$(H_2P)_n$ electrode more efficient, thus resulting in an improved photocurrent generation. We did not scan beyond potentials greater than +0.3 V *vs.* SCE since the electrochemical oxidation of iodide interferes with the photocurrent measurement.

The photocurrent action spectra of OTE/TiO_2/$(H_2P)_n$ electrode at different applied potentials are shown in Fig. 6. The IPCE values were calculated by normalizing the photocurrent values for incident light energy and intensity.[29] The action spectra show the maximum at 440 nm and 610 nm corresponding to the Soret and Q-bands respectively. This photocurrent response though broad in nature, match the absorption spectrum of the H_2P cluster film recorded in Fig. 2. These results

further confirm that the photocurrent originates from the excitation of the H_2P clusters.

Fig. 6

A maximum IPCE value of 2.0 % was obtained for OTE/TiO_2/$(H_2P)_n$ at an applied potential of 0.2 V *vs.* SCE. Such an enhanced IPCE value as compared with other two systems (no bias and 0 V *vs.* SCE) results from the increased transport rate of charge carriers at positive bias potentials. At a wavelength below 400 nm, direct excitation of TiO_2 film dominates and hence we couldn't resolve the photocurrent generation.

Mechanism of photocurrent generation

Efforts have been made in the past to employ porphyrin derivatives to sensitize TiO_2 electrodes.[14,15,30-36] A monolayer assembly of porphyrins attached to TiO_2 has been found to be effective in generating photocurrent under visible excitation. In the present study, we have deposited a cluster assembly of H_2P on nanostructured TiO_2 film. As shown in the previous section, these assembles are quite robust and absorb quite strongly in the visible region. The mechanism with which the photocurrent is generated in these films will either be (i) charge injection from the excited H_2P clusters into TiO_2 nanocrystallites or (ii) photoreduction of H_2P clusters in presence of iodide, followed by electron transfer from the reduced H_2P clusters to TiO_2 electrode. If the later mechanism is true we should not observe any

photoelectrochemical response when we exclude the electrolyte. Fig. 7 shows the photovoltage response of electrode under visible light irradiation.

Fig. 7

The fact that we observe photovoltage even in the absence of the redox couple, suggests a charge injection mechanism to be operative as illustrated by the reactions [eqns. (1)-(4)]. As discussed in the mechanism of photochemical solar cells[14], the photoexcitation of the sensitizer causes initial charge separation with electrons being injected into the semiconductor particle. Hence the observed photovoltage corresponds to the photoinduced charge injection process.

$$OTE/TiO_2/(H_2P)_n + h\nu \longrightarrow OTE/TiO_2/(H_2P)_n^*(S_1) \quad (1)$$

$$OTE/TiO_2/(H_2P)_n^* \longrightarrow OTE/TiO_2/(H_2P)_n + h\nu' \quad (2)$$

$$OTE/TiO_2/(H_2P)_n^* \longrightarrow OTE/TiO_2(\mathbf{e}^-)/(H_2P)_n^+ \quad (3)$$

$$2\ OTE/TiO_2/(H_2P)_n^+ + 3I^- \longrightarrow 2\ OTE/TiO_2/(H_2P)_n + I_3^- \quad (4)$$

The excited state oxidation potential of H_2P ($^1H_2P^*/H_2P^+$ = -0.7 V *vs.* NHE) is more negative than the TiO_2 conduction band (E_{CB} = -0.5 V *vs*. NHE),[37] thus facilitating the charge transfer from the excited state [eqn. (3)]. The oxidized H_2P (H_2P/H_2P^+ = 1.2 V *vs.* NHE)[38] counterpart reacts with iodide (I_3^-/I^- = 0.5 V *vs.* NHE)[10b,11] to generate the sensitizer [eqn. (4)]. The electrons transferred to the semiconductor nanocrystallites are collected at the OTE surface and are driven to the counter electrode through an

external circuit to regenerate the redox couple. The scheme illustrated in Fig. 8 summarizes the photoinduced processes leading to the generation of photocurrent at an OTE/TiO_2/$(H_2P)_n$ electrode.

The IPCE values observed for the sensitization of TiO_2 films by H_2P clusters is relatively low compared to the sensitized photocurrent generation using monomeric forms of porphyrin derivatives. For example, the TiO_2 electrodes modified tetra(4-carboxyphenyl)porphyrin exhibit incident photon-to-current conversion efficiency upto 55% at the Soret peak and 25-45% at the Q-band peaks.[15b] On the other hand, when TiO_2 electrodes were functionalized with porphyrin dimers (zinc porphyrin and free base porphyrin) an energy transfer route was found to compete with the charge injection pathway during the deactivation of zinc porphyrin.[34] Such an energy loss mechanism results in decreased IPCE performance as evident from the results discussed in the present study. Efforts are underway to incorporate electron donors within the H_2P clusters and improve the photoconversion efficiency of porphyrin cluster based nanoassemblies.

Fig. 8

Conclusion

Nanostructured thin films of porphyrin clusters have been prepared by assembling them on a TiO_2 electrode under the influence of a dc field. H_2P nanoclusters prepared in a acetonitrile/toluene mixed solvent exhibit a broad absorption in the Soret and Q-band regions that are different from the monomeric

H_2P. The nanostructured H_2P film has a broader absorption in the visible region as compared with H_2P clusters in mixed solvent and exhibit remarkable photosensitivity. Light energy harvesting application of these cluster film was demonstrated by employing them as a photoanode in the operation of a photoelectrochemical cell. The ability to utilize a wide spectral range of the solar spectrum resulting from the increased molar absorptivity in the visible region is a key feature of the porphyrin cluster based photoelectrochemical cell. Future efforts are aimed at improving the photoconversion efficiency of these molecularly engineered nanoassemblies.

Acknowledgment

This work was partially supported by a Grant–in–Aid (No. 13440216, 13555247, 11228205) and the Development of Innovative Technology (No. 12310) from the Ministry of Education, Culture, Sports, Science, and Technology, Japan, and for Scientific Research (21COE on Osaka University and Kyoto University Alliance for Chemistry). T.H. thanks to a 21st Century COE program of Osaka University for financial support during his stay at Notre Dame Radiation laboratory. PVK acknowledges the support from the Office of Basic Energy Science of the U. S. Department of the Energy. This is contribution No. NDRL 4464 from the Notre Dame Radiation Laboratory and from Osaka University.

.

References

1. (a) G. M. Whitesides, J. P. Mathias and C. T. Seto, *Science*, 1991, **254**, 1312. (b) N. B. Bowden, M. Weck, I. S. Choi, and G. M. Whitesides, *Acc. Chem. Res*., 2001, **34**, 231.
2. Special section on *"Supramolecular Chemistry and Self-Assembly*", *Science,* 2002, **295**, 2395.
3. D. G. Lidzey, D. D. C. Bradley, A. Armitage, S. Walker and M. S. Skolnick, *Science*, 2000, **288**, 1620.
4. (a) U. Siggel, U. Bindig, C. Endish, T. Komatsu, E. Tsuchida, J. Voigt, J.-H. Fuhrhop, *Ber. Bunsenges. Phys. Chem.*, 1996, **12**, 2070. (b) J.-H. Fuhrhop, U. Bindig and U. Siggel, *J. Am. Chem. Soc.,* 1993, **115**, 11036.
5. (a) J. R. Fredericks and A. D. Hamilton, *Hydrogen Bonding Control of Molecular Self-Assembly: Recent Advances in Design, Synthesis, and Analysis. In Comprehensive Supramolecular Chemistry*; ed. J.-P. Sauvage and M. W. Hosseini, Pergamon Press, Oxford, 1996, Vol. IX, Chapter 16. (b) T. van. Der. Boom, R. T. Hayes, Y. Zhao, P. J. Bushard, E. A. Weiss and M. R. Wasielewski, *J. Am. Chem. Soc.,* 2002, **124**, 9582. (c) X. Gong, T. Milic, C. Xu, J. D. Batteas and C. M. Drain, *J. Am. Chem. Soc.,* 2002, **124**, 12490.
6. W. West and B. H. Carroll, *In The Theory of Photographic Processes*, 3rd ed., ed. T. H. James, The McMillan Company, New York, 1966, Chapter 12.
7. T. Kobayashi, *J-Aggregates*, World Scientific, Singapore, 1996.
8. (a) Y-S. Kim, K. Liang, K-Y. Law and D. G. Whitten, *J. Phys. Chem.,* 1994, **98**, 984. (b) S. Barazzouk, H. Lee, S. Hotchandani and P. V. Kamat, *J. Phys. Chem. B,* 2000, **104**, 3616.
9. (a) D-G. Wu, Y-Y. Huang, C-H. Huang and L-B. Gan, *J. Chem. Soc., Faraday Trans.,* 1998, **94**, 1411. (b) D-G. Wu, C-H. Huang, L-B. Gan and Y-Y. Huang,

Langmuir, 1998, **14**, 3783. (c) Y. Majima, Y. Kanai and M. Iwamoto, *J. Appl. Phys*., 1992, **72**, 1637. (d) J. H. Yang, Y. M. Chen, Y. L. Ren, Y. B. Bai, Y. Wu, Y. S. Jang, Z.M. Su, W. S. Yang, Y .Q. wang, B. Zao, T. J. Li, *J. Photochem. Photobiol. A*, 2000, **134**, 1.

10. (a) C. Nasr, D. Liu, S. Hotchandai and P. V. Kamat, *J. Phys. Chem.,*1996, **100**, 11054. (b) P. V. Kamat, S. Barazzouk, K. G. Thomas and S. Hotchandani, *J. Phys. Chem. B*, 2000, **104**, 4014.
11. P. V. Kamat, S. Barazzouk, S. Hotchandani and K. G. Thomas. *Chem. Eur. J*., 2000, **6**, 3914.
12. P. K. Sudeep, B. I. Ipe, K. G. Thomas, M. V. George, S. Barazzouk, S. Hotchandai and P. V. Kamat, *Nano. Lett*., 2002, **2**, 29.
13. W. Kuhlbrandt, *Nature*, 1995, **374**, 497.
14. (a) A. Hagfeldt and M. Grätzel, *Acc. Chem. Res*., 2000, **33**, 269. (b) B. O'Regan and M. Grätzel, *Nature,* 1991, **353**, 737.
15. (a) G. K. Boschloo and A. Goossens, *J. Phys. Chem.,*1996, **100**, 19489. (b) S. Cherian and C. C. Wamser, *J. Phys. Chem. B,* 2000, **104**, 3624. (c) F. Fungo, L. Otero, E. N. Durantini, J. J. Silber and L. E. Sereno, *J. Phys. Chem. B,* 2000, **104**, 7644.
16. A. K. Burrell, D. L. Officer, P. G. Plieger and D. C. W. Reid, *Chem. Rev*., 2001, **101**, 2751.
17. D. Gust, T. A. Moore and A. L. Moore, *Acc. Chem. Res.,* 2001, **34**, 40.
18. Y. H. Kim, D. H. Jeong, D. Kim, S. C. Jeoung, H. S. Cho, S. K. Kim, N. Aratani and A. Osuka, *J. Am. Chem. Soc.,* 2001, **123**, 76.
19. A. Tsuda and A. Osuka, *Science*, 2001, **293**, 79.
20. S. Barazzouk, S. Hotchandani and P. V. Kamat, *Adv. Mater*., 2001, **13**, 1614.
21. H. Imahori, K. Tamaki, Y. Araki, Y. Sekiguchi, O. Ito, Y. Sakata and S. Fukuzumi, *J. Am. Chem. Soc.,* 2002, **124**, 5165.

22. V. Subramanian, E. Wolf and P.V. Kamat, *J. Phys. Chem. B*, 2001, **105***,* 11439.

23. (a) R.F. Pasternack, P.R. Huber, P. Boyd, G. Engasser, L. Francesconi, E. Gibbs, P. Fasella, G.C. Venturo, and L.d. Hinds, *J. Am. Chem. Soc.*, 1972, **94**, 4511. (b) A.S.R. Koti and N. Periasamy, *Chem. Mater.*, 2003, **15**, 369.

24. N. Micali, A. Romeo, R. Lauceri, R. Purrello, F. Mallamace and L. M. Scolaro, *J. Phys. Chem. B,* 2000, **104**, 9416.

25. N. Micali, F. Mallamace, A. Romeo, R. Purrello and L. M. Scolaro, *J. Phys. Chem. B,* 2000, **104**, 5897.

26. F. Mallamace, N. Micali, A. Romeo and L. M. Scolaro, *Colloid & Interface Science*, 2000, **5**, 49.

27. R. F. Pasternack, C. Fleming, S. herring, P. J. Collings, J. dePaula, G. deCastro and E. J. Gibbs*, Biophys. J.*, 2000, **79**, 550.

28. N. C. Maiti, S. Mazumdar and N. Periasamy, *J. Phys. Chem. B,* 1998, **102**, 1528.

29. I. Bedja, S. Hotchandai and P. V. Kamat, *J. Phys. Chem.,* 1994, **98**, 4133.

30. K. Kalyanasundaram, N. Vlachopoulos, V. Krishnan, A. Monnier and M. Grätzel, *J. Phys. Chem.*, 1987, **91**, 2342.

31. T. J. Schaafsma, *Sol. Energy Mater. Sol. Cells*, 1995, **38**, 349.

32. L. Otero, H. Osora, W. Li and M. A. Fox, *J. Porphyrins Phthalocyanines*, 1998, **2**, 123.

33. H. Mao, H. Deng, P. H. Li, Y. Shen, Z. Lu and H. Xu, *J. Photochem. Photobiol., A*, 1998, **114**, 209.

34. R. B. M. Koehorst, G. K. Boschloo, T. J. Savenije, A. Goossens and T. J. Schaafsma, *J. Phys. Chem. B*, 2000, **104** , 2371.

35. S. Cherian and C. C. Wamser, *J. Phys. Chem. B*, 2000, **104**, 3624.

36. T. M. R. Viseu, G. Hungerford and M. I. C. Ferreira, *J. Phys. Chem. B*, 2002, **106**, 1853.

37. K. Vinodgopal and P. V. Kamat, *Sol. Energy Mater. Sol. Cells,* 1995, **38**, 401.

38. H. Imahori, Y. Mori, and Y. Matano, *J. Photochem. Photobiol. C,* 2003, **4**, 51.

Figure Captions

Fig. 1. Absorption spectra of H_2P in its monomer and cluster forms prepared in (a) 0.02 mmol dm^{-3} in toluene and (b) 0.75 mmol dm^{-3} in acetonitrile/toluene (9/1, v/v), respectively . The absorption peaks at the Soret band are normalized for comparison.

Fig. 2. TEM images of H_2P clusters prepared using different compositions of acetonitrile and toluene in the ratio of (a) 3:1 v/v (0.75 mmol dm^{-3}) and (b) 9:1 v/v (0.75 mmol dm^{-3}), respectively.

Fig. 3. Absorption spectra of H_2P clusters deposited on OTE/TiO_2 electrodes; deposition time: (a) 0.5 min, (b) 1 min, (c) 2 min, (d) 5 min, (e) 8 min, and (f) 10 min. A dc voltage of 500 V was applied between OTE and OTE/TiO_2 electrodes immersed in 0.75 mmol dm^{-3} H_2P cluster solution in acetonitrile/toluene (9/1, v/v). The inset shows the growth of the film as monitored from an increase in absorbance at 410 nm.

Fig. 4. AFM images of H_2P nanocrystallites deposited on TiO_2 electrodes; (a) top view and (b) side view.

Fig. 5. (a) Photocurrent generation at an OTE/TiO_2/$(H_2P)_n$ electrode under illumination of white light (λ > 370 nm); electrolyte: 0.5 mol dm^{-3} NaI and 0.01 mol dm^{-3} I_2 in acetonitrile. Input power; 110 mW cm^{-2}. (b) I-V characteristics of an OTE/TiO_2/$(H_2P)_n$ electrode under illumination of white light (λ > 370 nm);

electrolyte: 0.5 mol dm^{-3} NaI and 0.01 mol dm^{-3} I_2 in acetonitrile. Input power; 110 mW cm^{-2}.

Fig. 6. Photocurrent action spectra (IPCE versus wavelength) of an OTE/TiO_2/$(H_2P)_n$ electrode (a) with no applied bias potential and at an applied bias potential of (b) 0 V and (c) 0.2 V *vs.* SCE. The photoresponse of OTE/TiO_2 electrode under no applied bias is also shown for comparison (d).

Fig. 7. Photovaltage generation at OTE/TiO_2 and OTE/TiO_2/$(H_2P)_n$ electrodes in an acetonitrile solution containing 0.1 mol dm^{-3} *n*-tetrabuthylammonium perchlorate (TBAP) under deaerated and oxygenated conditions.

Fig. 8. Energy diagram for photocurrent generation at an OTE/TiO_2/$(H_2P)_n$ electrode.

Fig. 1

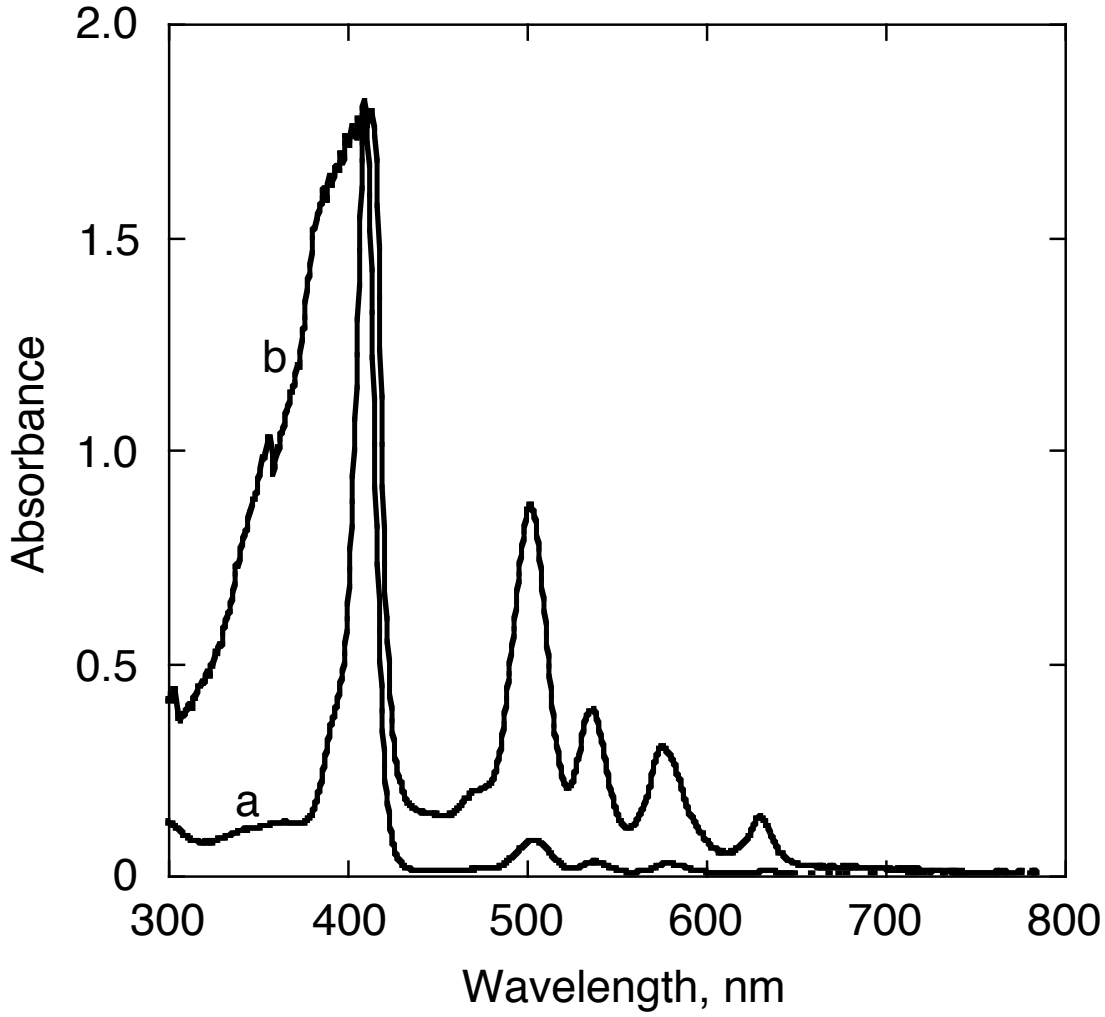
2.0
1.5
1.0
0.5
0
Absorbance
b
a
300
400
500
600
700
800
Wavelength, nm

Fig. 2

(a)

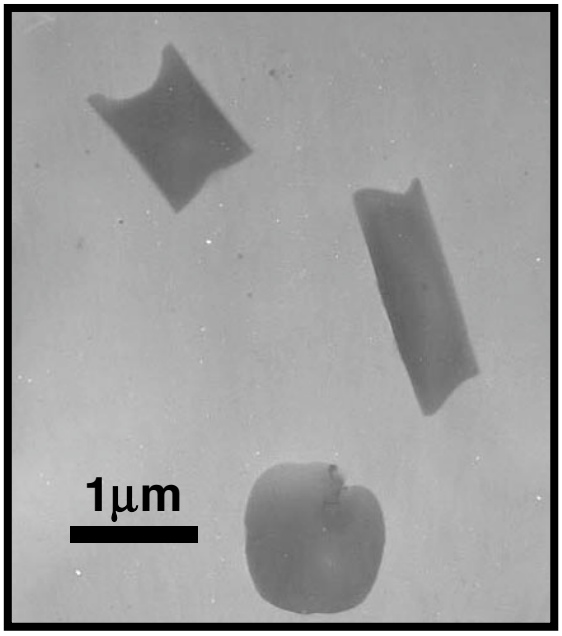

(b)

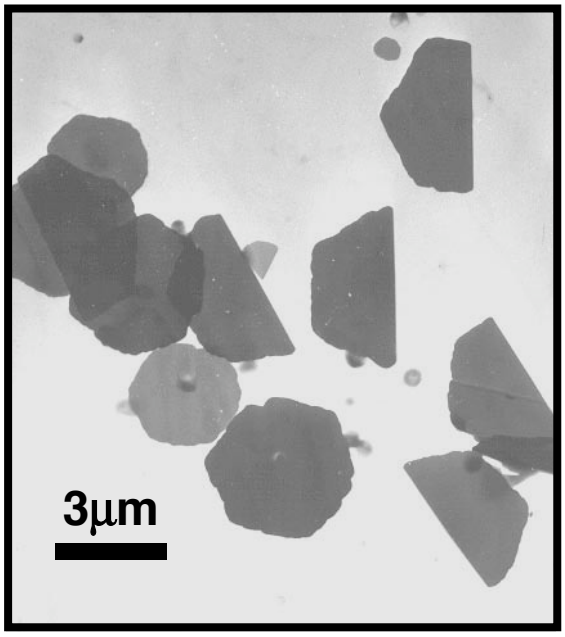

Fig. 3

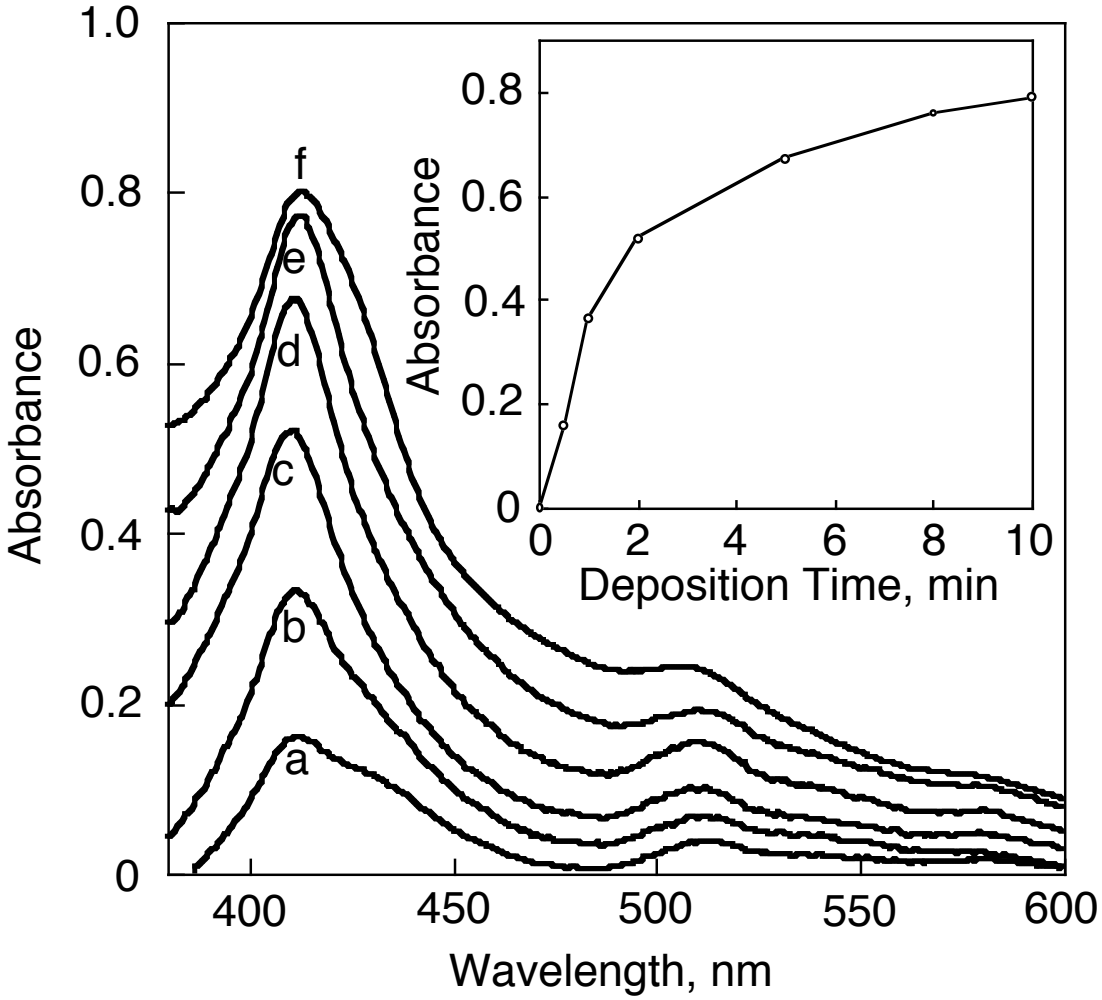
1.0
0.8
0.6
0.4
0.2
0
Absorbance
400
450
500
550
600
Wavelength, nm
f
e
d
c
b
a
0.8
0.6
0.4
0.2
0
Absorbance
0
2
4
6
8
10
Deposition Time, min

Fig. 4

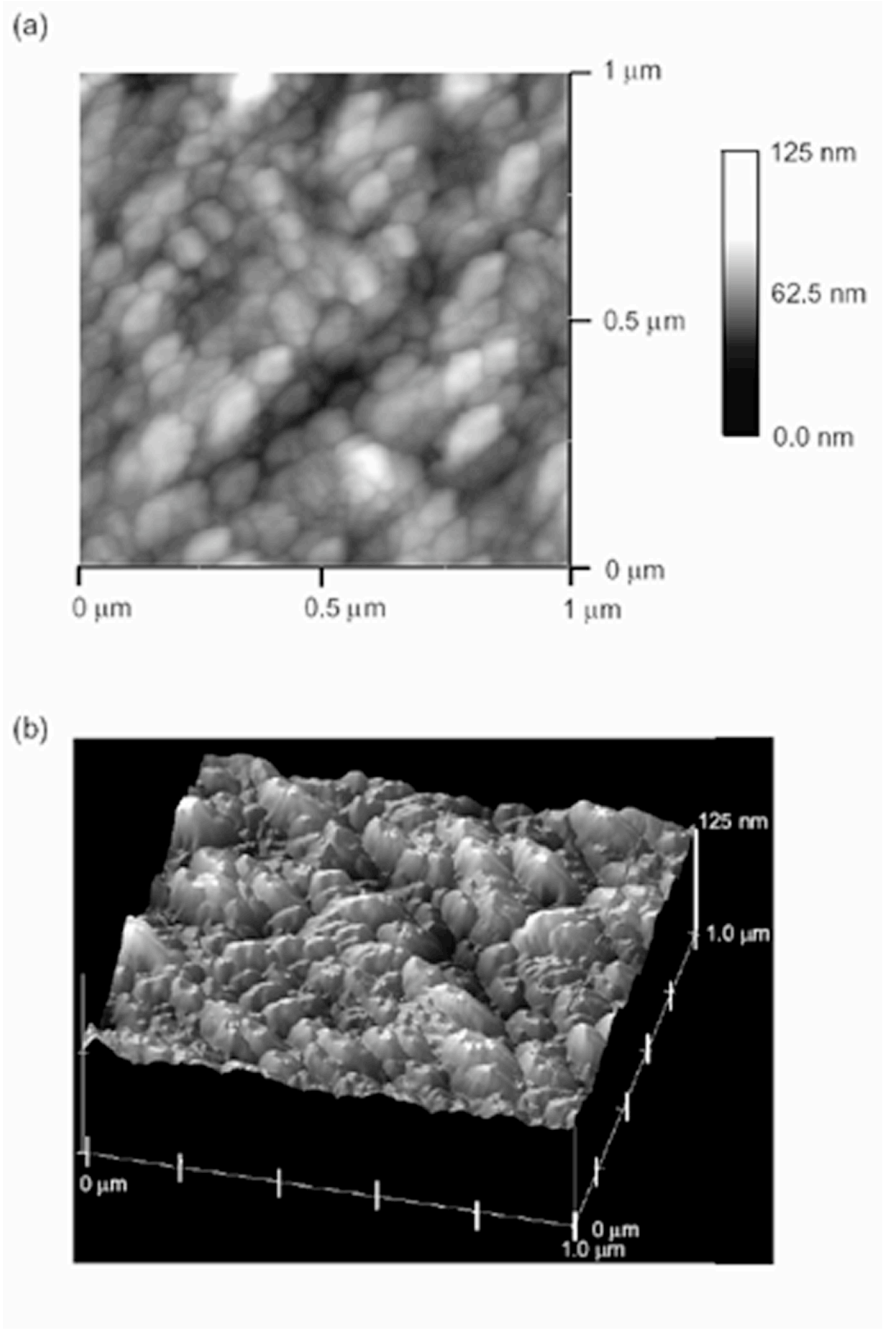
(a)
1 μm
0.5 μm
0 μm
0 μm
0.5 μm
1 μm
125 nm
62.5 nm
0.0 nm
(b)
125 nm
1.0 μm
0 μm
0 μm
1.0 μm

Fig. 5

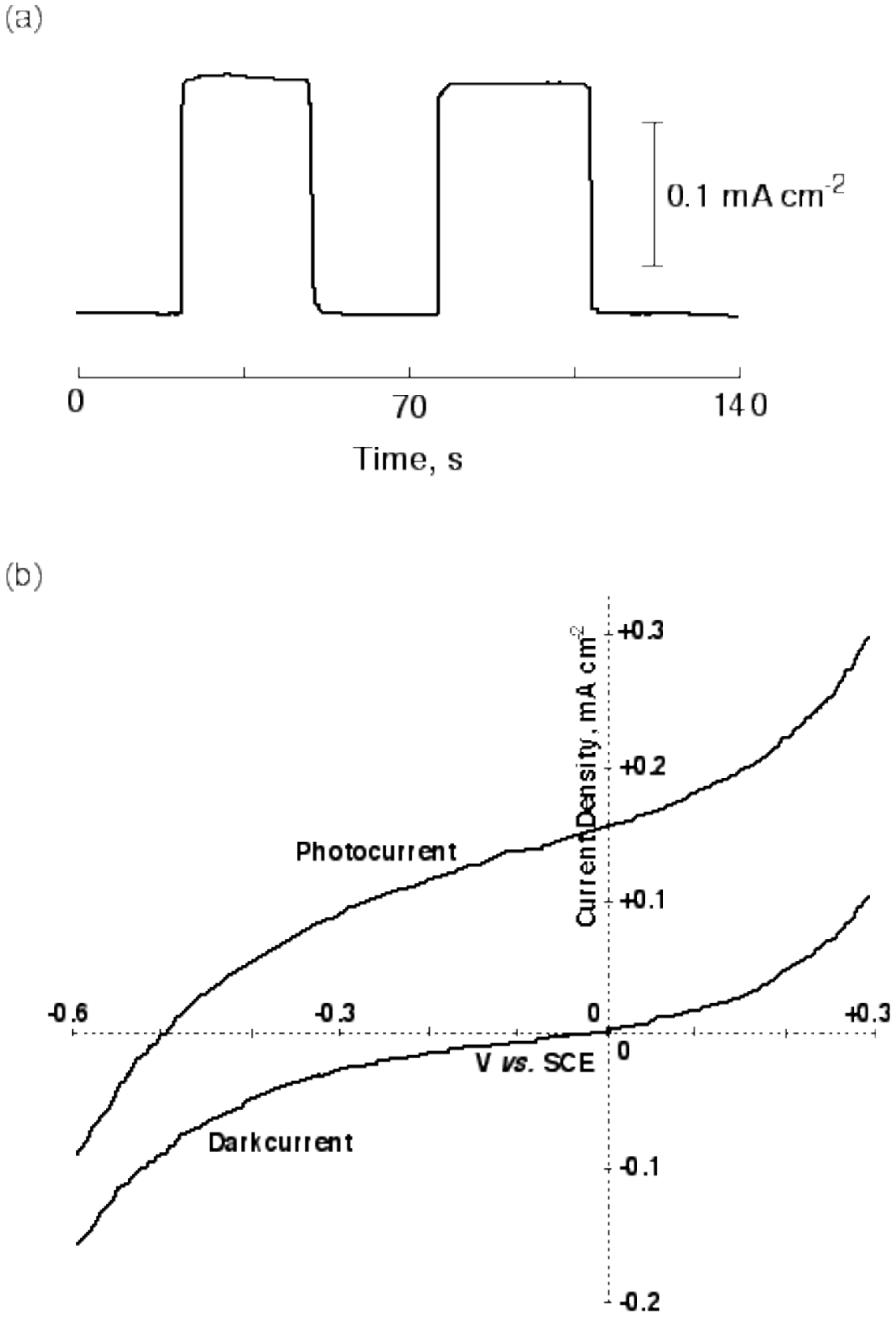
(a)
0.1 mA cm-2
0
70
140
Time, s
(b)
Current Density, mA cm-2
+0.3
+0.2
+0.1
-0.1
-0.2
Photocurrent
Darkcurrent
-0.6
-0.3
0
+0.3
V vs. SCE

Fig. 6

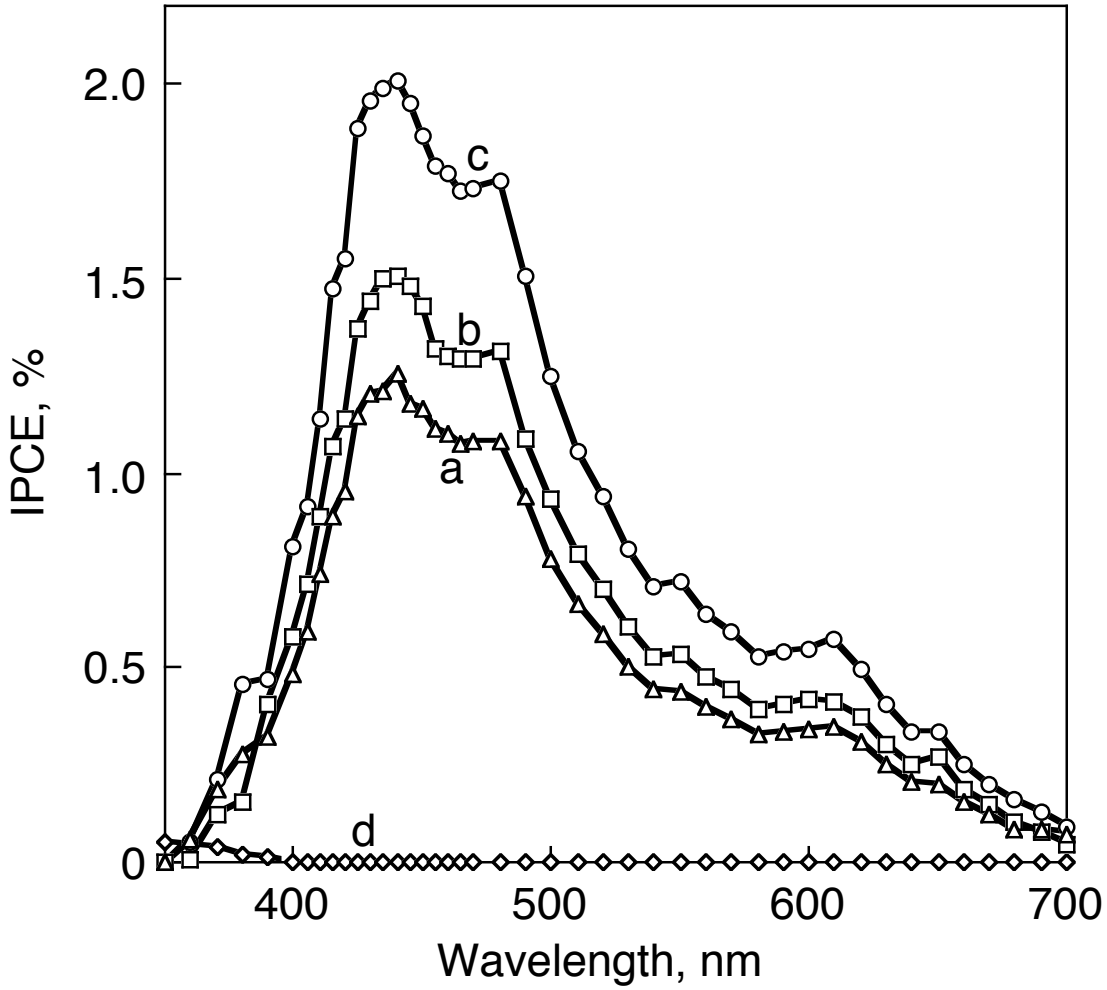

Fig. 7

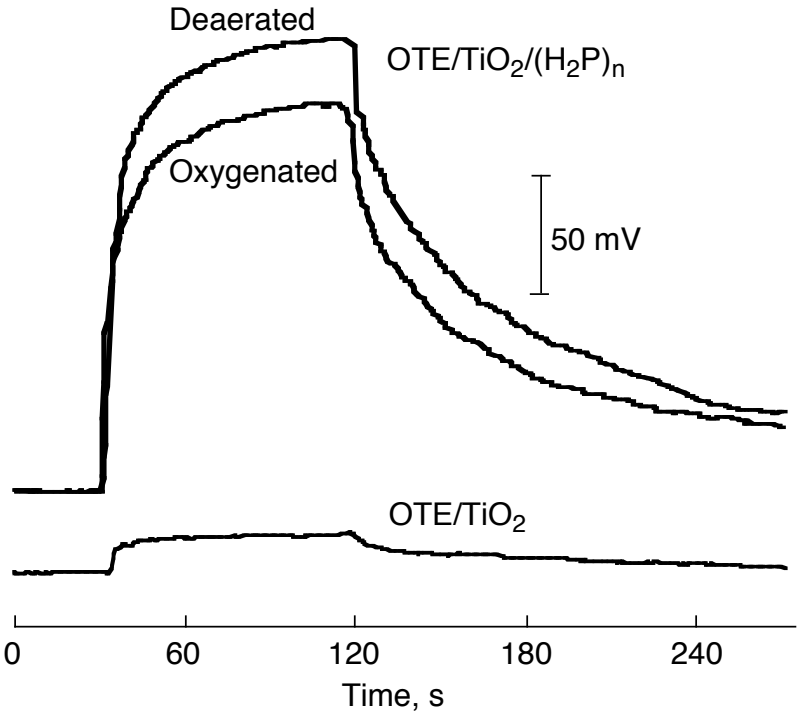
Deaerated
OTE/TiO2/(H2P)n
Oxygenated
50 mV
OTE/TiO2
0
60
120
180
240
Time, s

Fig. 8

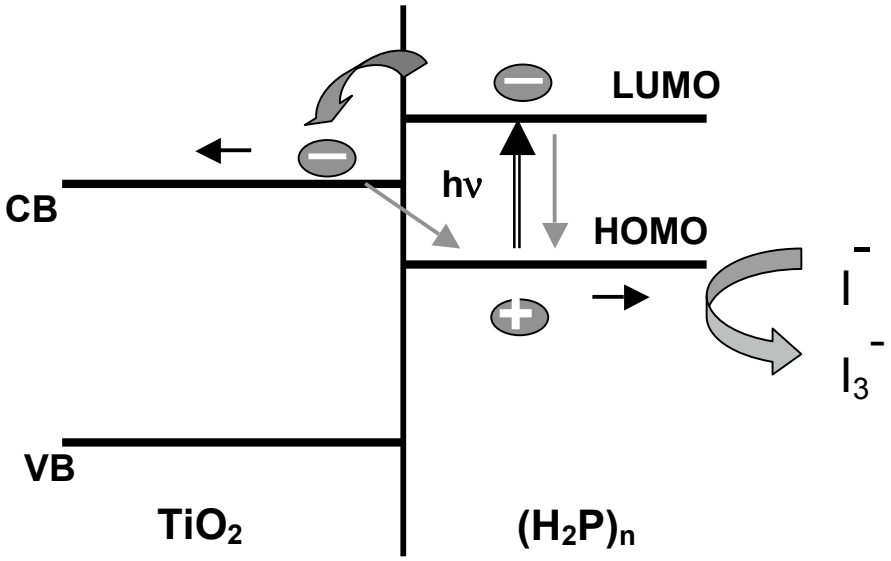

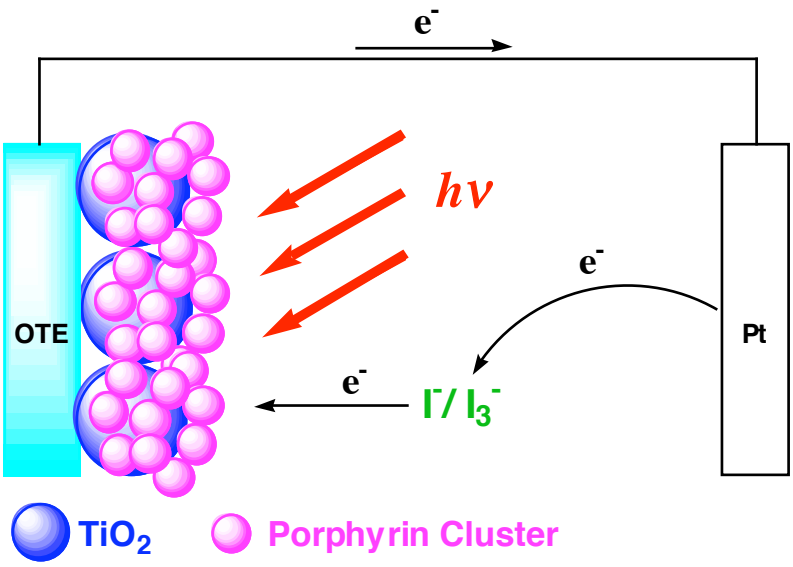

OTE: Optically Transparent Electrode

Nanostructured thin films of porphyrin clusters prepared by assembling them on a TiO_2 electrode under the influence of a dc field exhibits remarkable photosensitivity in visible region.